American Mineralogist, Volume 77, pages 565–576, 1992

Diffusive reequilibration of melt and fluid inclusions

ZHENWEI QIN, FANGQIONG LU, ALFRED T. ANDERSON, JR.
Department of the Geophysical Sciences, University of Chicago, 5734 South Ellis Avenue, Chicago, Illinois 60637, U.S.A.

ABSTRACT

A mathematical model is presented that investigates the diffusive reequilibration of chemical species in melt inclusions with external melt through the host crystal. Analytic solution of the differential equations reveals that reequilibration is easier (1) for species with higher diffusivities in the host crystal, (2) for species with higher partition coefficients (k) between host crystal and melt (but reequilibration rates become insensitive to the increase in k after k exceeds about 0.1), and (3) for smaller-sized host crystals and melt inclusions. Less than 2 yr are required for H_2O in a rhyolitic melt inclusion 25 μm in radius located at the center of a quartz crystal 1 mm in radius to reach 95% reequilibration with external melt, if the diffusion coefficient of H_2O in quartz = 10^{-10} cm^2/s at 800 °C and the partition coefficient = 10^{-4}. This cautions against the use of H_2O content in a melt inclusion to represent the H_2O contents in the magma when the inclusion formed. The H_2O contents in melt inclusions in quartz will reflect their original values if the H_2O contents of the magma remain constant and if the materials are quickly erupted and cooled. Rhyolitic melt inclusions from the late-erupted, crystal-rich Bishop Tuff, although variable in their content of low-diffusivity trace elements, have relatively low and uniform H_2O contents, consistent with diffusive reequilibration of inclusions with the late-stage, H_2O-poor magmas shortly before eruption. Because diffusive exchange becomes more sluggish as the partition coefficient decreases, melt inclusions in olivine and orthopyroxene are expected to preserve better the original concentrations of many incompatible elements (REEs, Rb, Cs, Ba, U, Th, etc.) than those in clinopyroxene. For the same melt inclusion, highly incompatible elements are expected to exchange more slowly than less incompatible or compatible elements.

The above model can also be applied to the diffusive leakage of H_2O from fluid inclusions in quartz. Small fluid inclusions (≤ 10 μm in radius) trapped at the center of a quartz crystal 1 mm in radius can effectively lose their H_2O in less than 50000 yr during retrograde decompression of metamorphic rocks at 500 °C, if the solubility and diffusivity of H_2O in quartz are 1 ppm/kbar and 10^{-13} cm^2/s. The preferential loss of H_2O can result in a significant increase in the CO_2/H_2O ratio in fluid inclusions.

INTRODUCTION

Melt inclusions are tiny bodies of glass (quenched melt) that are encased in volcanic phenocrysts. They have been used to study the differentiation (e.g., Roedder and Weiblen, 1970; Watson, 1976) and mixing and degassing (e.g., Anderson and Wright, 1972; Anderson, 1976; Skirius et al., 1990) of magmas by many workers. Two important assumptions about melt inclusions have been (1) any melt initially trapped within a growing crystal is representative of the melt from which the crystal grew (Anderson, 1974; Watson, 1976); and (2) after entrapment, the melt may react with the host crystal, but diffusive exchange between trapped and external melts through the crystal is unimportant (Anderson, 1974; Watson, 1976).

The first assumption was challenged by Watson et al. (1982). They suggested that the composition in the melt adjacent to a growing crystal may be different from the average melt because of the selective incorporation of certain elements by the crystal. In particular, highly incompatible elements are rejected by the growing crystal and hence may accumulate in a boundary layer of melt adjacent to the phenocryst (see also Albarede and Bottinga, 1972). Many trace elements have low diffusivities, and thus the compositional anomalies of the boundary layer cannot be ignored (Bacon, 1989); these elements include P, Ti, Zr, Ba, Mn, etc., with diffusivities in rhyolite at 800 °C on the order of 10^{-10} to 10^{-11} cm^2/s (see compilation by Bacon, 1989). For components such as H_2O, with diffusivities in rhyolitic melt as high as 10^{-7} to 10^{-6} cm^2/s at 800 °C (Karsten et al., 1982; Lapham et al., 1984), the accumulation effect in the boundary layer is probably negligible. In general, boundary layer accumulation is probably negligible for trace elements with diffusivities significantly larger than those of major elements (e.g., Si and Al) that may control the rate of crystal growth (Lu, 1991).

The second assumption may be questioned in view of

0003–004X/92/0506–0565$02.00

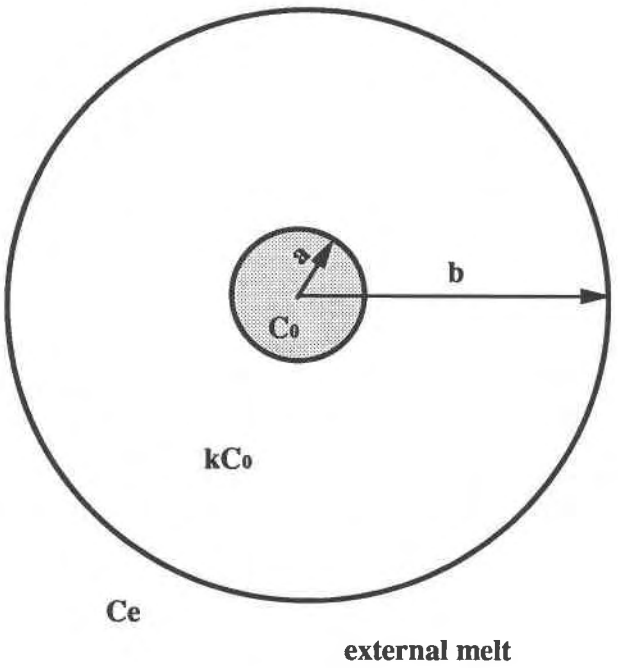

Fig. 1. A melt inclusion of radius a enclosed in the center of a crystal of radius b. Initially, the concentrations of a certain chemical species in the inclusion and the crystal are C_0 and kC_0, respectively, where k is the partition coefficient of the species between crystal and melt. The crystal is later brought into contact with a new melt with a concentration of the species = C_e. As $C_e \neq C_0$, exchange of this species occurs between the trapped and the external melts by diffusion across the crystal.

work by Roedder (1981), Hall et al. (1991), and others on fluid inclusions and by Roeder and Campbell (1985) and Scowen et al. (1991) on mineral inclusions. For example, Roedder (1981) suggested that CO_2-rich fluid inclusions in quartz from some granulites may be due to the diffusive loss of H_2O from the inclusions during retrograde metamorphism, whereas Scowen et al. (1991) showed that the compositions of chromite inclusions in olivine phenocrysts from Kilauea Iki lava lake, Hawaii, changed significantly during 22 yr of diffusive exchange through host crystals with surrounding interstitial melt.

If diffusive reequilibration is important for fluid and mineral inclusions, then it may be also important for melt inclusions. In this paper, a mathematical model of the diffusive reequilibration of melt inclusions with external melt will be developed. Based on the model results, the H_2O content in melt inclusions in quartz in general is discussed and is applied to Bishop Tuff rhyolites. The model can also be applied to fluid inclusions after some appropriate modification.

The mathematical model and its solution

Formulating the problem

Consider a spherical crystal of radius b with a melt inclusion of radius a at the center (Fig. 1) and an arbitrary chemical species i. The crystal and the melt inclusion formed earlier in a magma with concentration C_0 of i. The crystal is later brought into contact with a new melt characterized by a concentration C_e of i that is different from C_0. As $C_e \neq C_0$ and as the external melt is far more abundant, the concentration of this species in the inclusion tends to approach the external concentration C_e by means of the diffusion of this species through the crystal.

Notation

C_0: initial concentration in melt inclusion
C_e: concentration in the exterior melt in contact with the host crystal
$C(r,t)$: concentration in the crystal, which is a function of time and position
$C_1(t)$: concentration in melt inclusion, which is a function of time
a: radius of melt inclusion
b: radius of host crystal
r: radial coordinate variable
t: time variable
D: diffusion coefficient of the species in the crystal
k: partition coefficient of the species between crystal and melt
ρ_m: density of melt
ρ_c: density of crystal

Assumptions

1. The concentration in the new magma C_e is constant in space and time.

2. The concentration of the species in the outer surface of the host crystal at any moment $C(b,t)$ is in equilibrium with the magma; i.e., $C(b,t) = kC_e$. Similarly, the species in the inner surface of the crystal at any moment is in equilibrium with that of the melt inclusion: $C(a,t) = kC_1(t)$.

3. Diffusive flux across the inner surface is the only process that allows the concentration in the melt inclusion to change.

4. The species in the melt inclusion is uniformly distributed at all times.

5. The melt inclusion is at the center of a spherical crystal.

6. The effect of changing concentration on the density of the enclosed melt is negligible.

Assumption 1 is probably not true in many circumstances but is appropriate so long as the time during which C_e changes is much longer than that required for effective reequilibration. Assumption 2 is justified because the inner and outer surfaces of the host crystal are in direct contact with the respective melts. Assumption 3 limits the discussion to diffusive modification. Assumption 4 is consistent with the general knowledge that chemical diffusivities are generally greater in melts than in solids. Assumption 5 and 6 do not strictly fit the natural systems but are necessary approximations for the sake of theoretical treatment.

With assumption 3, we can write

$$\frac{d}{dt}\left[\frac{4}{3}\pi a^3 \rho_m C_I(t)\right] = 4\pi a^2 D \frac{\partial(\rho_c C)}{\partial r}\Big|_{r=a}. \quad (1)$$

This expresses the condition that the rate of change of the total amount of a species in the melt inclusion is determined by the diffusive flux of the species across the inner surface.

The concentration gradient at the inner surface of the host crystal appearing in Equation 1 can be evaluated by solving the following diffusion equation in the host crystal:

$$\frac{\partial C}{\partial t} = D\left(\frac{\partial^2 C}{\partial r^2} + \frac{2}{r}\frac{\partial C}{\partial r}\right) \qquad a < r < b. \quad (2)$$

This is a diffusion equation for an isotropic medium in a spherical coordinate system (e.g., Carslaw and Jaeger, 1959).

The initial condition is

$$C(r,0) = kC_0 \qquad a \le r \le b \quad (3)$$

i.e., the initial concentration of the species in the crystal is uniformly at equilibrium with that in the melt inclusion.

Two boundary conditions follow from assumption 2:

$$C(b,t) = kC_e \quad (4)$$

$$C(a,t) = kC_I(t). \quad (5)$$

Combining Equations 1 and 5 gives

$$\frac{dC(a,t)}{dt} = \beta \frac{D}{a}\frac{\partial C}{\partial r}\Big|_{r=a} \quad (6)$$

where

$$\beta = 3k\rho_c/\rho_m. \quad (7)$$

Table 1. The first six roots of $\tan(1 - a/b)q = \dfrac{(a/b)\beta q}{(aq/b)^2 - \beta}$

k	1	0.1	0.01	0.001	0.0001	0.00001
			a/b = 0.005			
q_1	3.142	3.142	3.141	3.140	3.108	1.188
q_2	6.283	6.283	6.282	6.271	3.801	3.160
q_3	9.425	9.425	9.422	9.349	6.332	6.316
q_4	12.566	12.566	12.559	11.638	9.481	9.473
q_5	15.708	15.707	15.692	12.957	12.636	12.630
q_6	18.850	18.847	18.819	15.887	15.792	15.787
			a/b = 0.01			
q_1	3.142	3.142	3.141	3.130	1.872	0.596
q_2	6.283	6.283	6.275	5.702	3.190	3.174
q_3	9.425	9.423	9.394	6.615	6.353	6.347
q_4	12.567	12.561	12.471	9.580	9.524	9.520
q_5	15.708	15.698	15.419	12.729	12.696	12.694
q_6	18.850	18.831	17.917	15.893	15.869	15.867
			a/b = 0.05			
q_1	3.142	3.131	2.929	1.203	0.385	0.122
q_2	6.285	6.191	4.127	3.332	3.309	3.307
q_3	9.430	9.053	6.771	6.625	6.615	6.614
q_4	12.579	11.643	10.007	9.928	9.922	9.921
q_5	15.733	14.290	13.288	13.233	13.228	13.228
q_6	18.892	17.231	16.582	16.539	16.535	16.535
			a/b = 0.1			
q_1	3.143	3.053	1.859	0.622	0.198	0.063
q_2	6.296	5.509	3.637	3.502	3.492	3.491
q_3	9.468	7.873	7.041	6.987	6.982	6.981
q_4	12.668	10.947	10.510	10.476	10.472	10.472
q_5	15.903	14.284	13.991	13.965	13.963	13.963
q_6	19.173	17.698	17.476	17.456	17.454	17.453

Note: $\beta = 3k(\rho_c/\rho_m)$, where k, ρ_c, and ρ_m are the partition coefficient and the densities of crystal and melt, respectively. In the calculation, is it assumed that $\rho_c/\rho_m = 1.2$.

Solving the problem

Equation 2 coupled with its initial condition (Eq. 3) and its boundary conditions (Eqs. 4 and 6) has to be solved to give $C(r,t)$. With this, the concentration of the species in the melt inclusion can be calculated from Equation 5. The solution for $k = 1$ and $C_e = 0$ was given by Carslaw and Jaeger (1959, p. 350, Eq. 24) for a heat conduction problem. The above, more general problem can be solved by the Laplace transformation method (see Appendix 1). The solution is

$$C(r,t) = kC_e + \frac{4\beta kb}{r}(C_0 - C_e) \times \sum_{n=1}^{\infty} \frac{\sin(1 - r/b)q_n \exp(-q_n^2 Dt/b^2)}{[2\beta(1-\alpha)q_n + 4\alpha q_n \sin^2(1-\alpha)q_n - \beta \sin 2(1-\alpha)q_n]} \quad (8)$$

where $\alpha = a/b$, and q_n ($n = 1, 2, 3 \ldots$) is the positive root of

$$\tan(1 - \alpha)q = \frac{\alpha\beta q}{\alpha^2 q^2 - \beta}. \quad (9)$$

There is an infinite number of roots for the transcendental equation (Eq. 9). The first six roots are compiled in Table 1 for selected values of α and β.

The concentration of the species in a melt inclusion is obtained by evaluating Equation 8 at $r = a$ and recalling that $C_I(t) = C(a, t)/k$. The resulting expression is

$$C_I(t) = C_e + \frac{4\beta}{\alpha}(C_0 - C_e) \times \sum_{n=1}^{\infty} \frac{\sin(1-\alpha)q_n \exp(-q_n^2 Dt/b^2)}{[2\beta(1-\alpha)q_n + 4\alpha q_n \sin^2(1-\alpha)q_n - \beta \sin 2(1-\alpha)q_n]}.$$

This can be further simplified (see Appendix 1) to become

$$C_I(t) = C_e + \frac{2\beta}{\alpha}(C_0 - C_e) \times \sum_{n=1}^{\infty} \frac{\exp(-q_n^2 Dt/b^2)}{\{\gamma q_n \sin[(1-\alpha)q_n] + [\alpha(1-\alpha)q_n^2 - \beta/\alpha]\cos[(1-\alpha)q_n]\}} \quad (10)$$

where $\gamma = [2\alpha + \beta(1 - \alpha)]$.

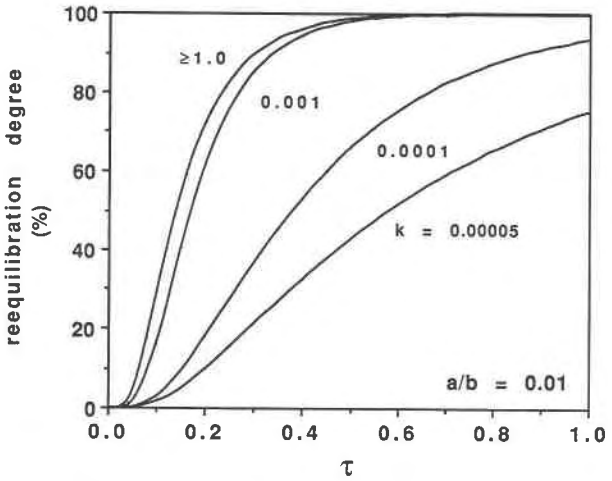

Fig. 2. The effects of partition coefficients. As the value of k decreases, the time it takes to achieve a given degree of reequilibration increases. Note that this effect is amplified rapidly when k becomes very small. On the other hand, it diminishes as k increases, and all curves with $k \geq \sim 1$ are essentially indistinguishable. Here, $a/b = 0.01$, where a and b are the radius of melt inclusion and host crystal, respectively. Dimensionless time is defined as $\tau = Dt/b^2$. Values on the curves are partition coefficients (k).

It is more convenient to express the results in terms of the extent of approach to reequilibration defined as

$$\phi = \frac{C_1(t) - C_0}{C_e - C_0}. \tag{11}$$

Thus, no exchange occurs when $\phi = 0$, and reequilibration is fully achieved when $\phi = 1$. Rearrangement of Equation 10 and substitution of Equation 11 yield

$$\phi(t) = 1 - \frac{2\beta}{\alpha} \times \sum_{n=1}^{\infty} \frac{\exp(-q_n^2 Dt/b^2)}{[\gamma q_n \sin(1-\alpha)q_n + [\alpha(1-\alpha)q_n^2 - \beta/\alpha]\cos(1-\alpha)q_n]}. \tag{12}$$

The rate of convergence of the infinite series in Equation 12 depends on the value of the nondimensionalized time Dt/b^2. The larger this value is, the faster the series converges. In general, this series converges very fast because of the factor of q_n^2 in the exponential. For example, even with the dimensionless time $\tau(= Dt/b^2)$ as small as 0.1, the second term in the series is on the order of 10^{-1} to 10^{-2}; the third term 10^{-4}, the fourth term 10^{-6} to 10^{-7}, the fifth term 10^{-10} to 10^{-11}, and so on. Thus, in using Equation 12 to calculate the reequilibration degree, a very good approximation (error $<1\%$) can be achieved by retaining only the first two terms of the series, even when τ is as small as 0.1. It can be shown that when $\tau \geq 0.5$, adequate accuracy (better than 99%) can be obtained by retaining only the leading term of the series in Equation 12, i.e.,

$$\phi(t) \approx 1 - \frac{1}{d_1}\exp(-q_1^2\tau) - \frac{1}{d_2}\exp(-q_2^2\tau) \tag{13a}$$

when $0.1 \leq \tau\ (= Dt/b^2) < 0.5$;

$$\phi(t) \approx 1 - \frac{1}{d_1}\exp(-q_1^2\tau) \tag{13b}$$

when $\tau \geq 0.5$ and where

$$d_i = \frac{\alpha}{2\beta}\{[2\alpha + \beta(1-\alpha)]q_i \sin(1-\alpha)q_i + [\alpha(1-\alpha)q_i^2 - \beta/\alpha]\cos(1-\alpha)q_i\} \tag{13c}$$

$i = 1, 2$; and β is given in Equation 7.

With Equations 13a, 13b, and 13c and Table 1, the degree of diffusive reequilibration can be computed easily using a calculator. To illustrate, consider the following case: $a = 10\ \mu$m, $b = 1$ mm ($\therefore\ \alpha = 0.01$), $k = 0.0001$, $D = 10^{-10}$ cm^2/s, $t = 1$ yr ($\therefore\ \tau = 0.315$). Then from Table 1, $q_1 = 1.8715$, $q_2 = 3.1903$. Substituting these values in Equation 13a yields $\phi = 40.6617\%$, which is essentially identical to the true degree of reequilibration of 40.6616% found by summing the series in Equation 12 to the tenth term (the tenth term is on the order of 10^{-40}). If $t = 2$ yr ($\therefore\ \tau = 0.630$), then Equation 13b can be used, which gives $\phi = 64.72\%$, which is identical to the true value. Given ϕ, one can obtain the new concentration of the species in the melt inclusion from

$$C_1 = \phi C_e + (1 - \phi) C_0. \tag{14}$$

Results and discussion

It can be seen from Equation 12 that the degree of reequilibration depends only on three parameters: the dimensionless time $\tau\ (= Dt/b^2)$, the ratio of the melt inclusion size over the host crystal size $a/b\ (= \alpha)$, and the partition coefficient k (contained in β). It follows that for a given a, b, and k, the time (t) needed to reach a given degree of reequilibration is inversely proportional to the diffusion coefficient. For example, if the diffusion coefficient decreases by a factor of 10, then the time it takes to reach a certain degree of reequilibration will increase by a factor of 10.

Equation 12 reveals that the extent of the approach to reequilibration is independent of the compositional difference between the original melt inclusion and the new external melt (i.e., $C_0 - C_e$). The absolute content of the species in the melt inclusion during the exchange process does depend on the original values, however (see Eq. 14).

Figures 2–4 show how the partition coefficient affects the rate of exchange of the species between melt inclusion and the melt outside the crystal. The smaller the value of k, the more sluggish is reequilibration. For example, for $a/b = 0.01$, 50% reequilibration ($\phi = 0.5$) takes about twice as long for $k = 10^{-4}$ as for $k = 10^{-3}$. The effect increases as a/b increases. Thus, for $a/b = 0.05$, the dif-

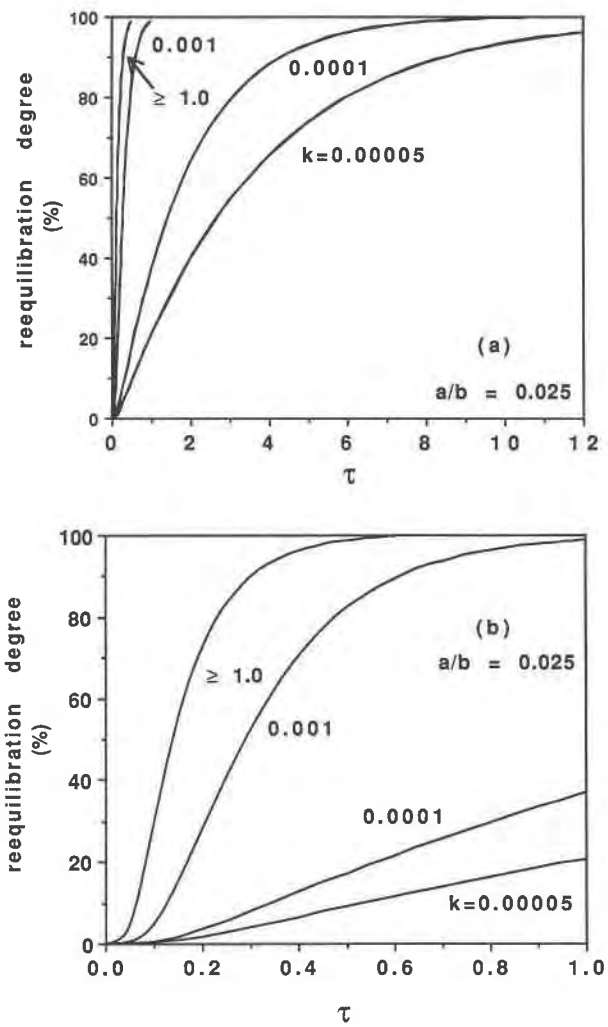

Fig. 3. (**a**) Same as Figure 2, but with $a/b = 0.025$. (**b**) Enlargement of **a**.

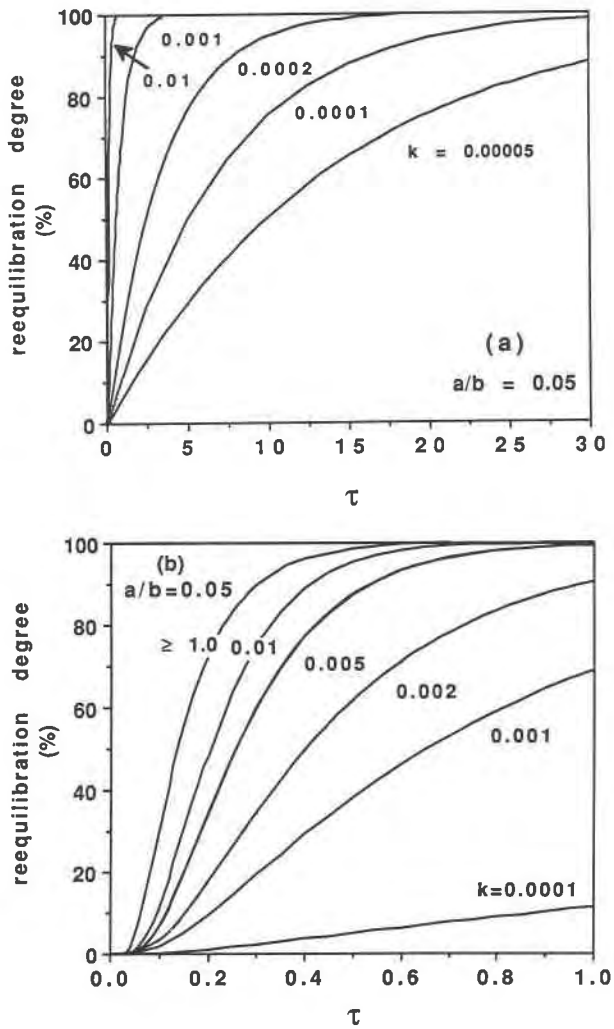

Fig. 4. (**a**) Same as Figure 2, but with $a/b = 0.05$. (**b**) Enlargement of **a**.

ference becomes 8 times as long. In the extreme case, when $k = 0$, the host crystal acts as a perfect insulator, protecting its inclusions from any diffusive exchange with the external melt. On the other hand, although it is generally true that the increase in k value reduces the time needed to achieve a given degree of reequilibration, the magnitude of this effect diminishes as k increases, until it reaches a limit beyond which any further increase in k results in no observable effect in the reduction of the equilibration time. Thus, in these figures, the curves for $k \geq \sim 1$ are essentially indistinguishable from one another because diffusive reequilibration under such conditions is primarily governed by diffusion in the crystal. The work by Scowen et al. (1991), by ignoring k, implicitly corresponds to the case of $k = 1$.

The effect of inclusion size is complex. On the one hand, for a given crystal size, an increase in the inclusion size results in an increase in the total amount of the species to be exchanged, thus adding to the time needed to achieve reequilibration. On the other hand, increase in the inclusion size (for a fixed crystal size) both reduces the distance for the species to travel and increases the inner surface area across which diffusive exchange occurs, thereby making it easier for the exchange to proceed. Figure 5 shows that, for a k value of 10^{-3}, as the ratio a/b increases, the dimensionless time it takes to reach a given degree of reequilibration also increases until this ratio reaches ~ 0.7, when the combined effect of the decreasing transfer distance and the increasing exchange area becomes dominant. If a/b exceeds 0.7, then diffusive reequilibration becomes more rapid, rather than slower, as the inclusion size increases. For most of, if not all, the natural samples, a/b is $\ll 0.7$. Thus, as melt inclusions become larger (i.e., as the ratio a/b increases), the extent of reequilibration typically becomes smaller. For example, for a species with $k = 10^{-3}$, it takes about 0.35 in the dimensionless time

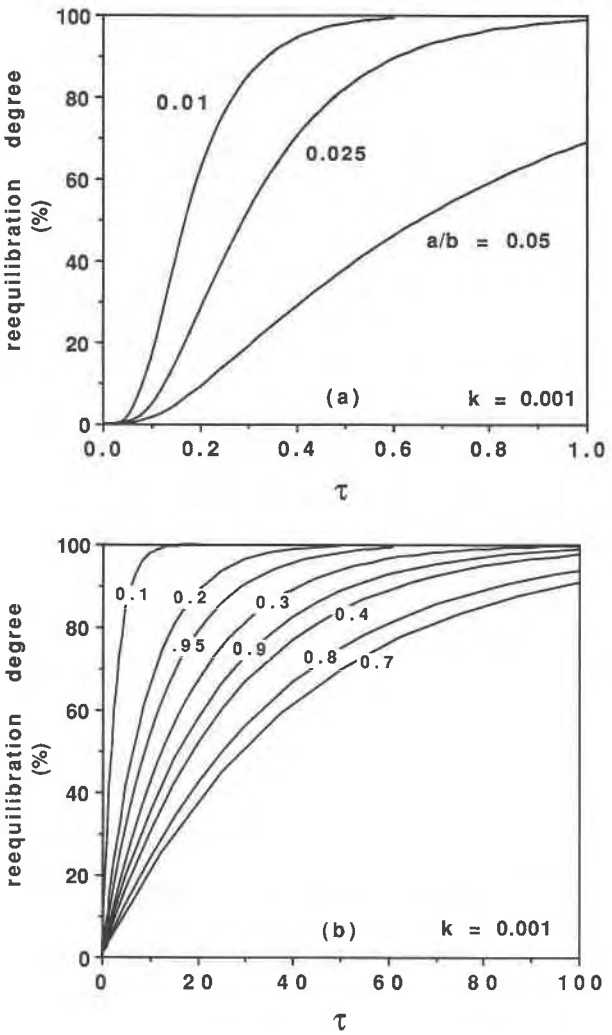

Fig. 5. The effect of inclusion size. (**a**) For a fixed crystal size, increasing the inclusion size increases the time needed to reach a given degree of reequilibration, as long as a/b is less than ~0.7. Values on the curves are a/b. (**b**) When $a/b >$ ~0.7, increasing the inclusion size will decrease the time needed to reach a given degree of reequilibration. See text for discussion. Values on the curves are a/b.

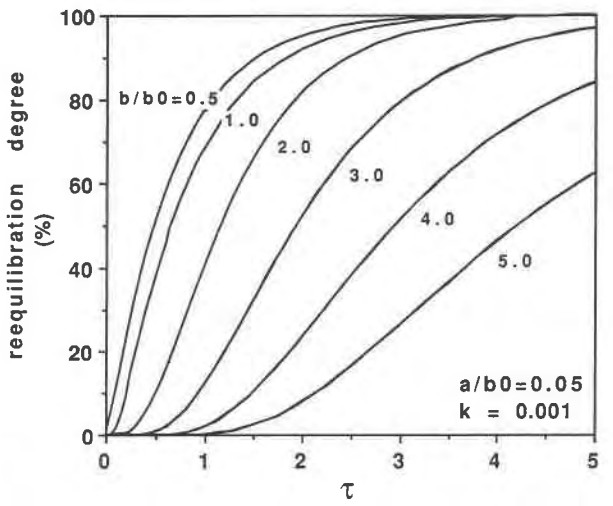

Fig. 6. The effect of host crystal size. For a given melt inclusion size, the larger the host crystal, the longer it takes to reach a given degree of reequilibration. But the time is not proportional to the square of the host crystal size, as might be expected. See text for discussion. Here, $\tau = Dt/b_0$; values on the curves are the ratio of b/b_0.

(i.e., $Dt/b^2 = 0.35$) to reach 90% of reequilibration if $a/b = 0.01$, compared to 1.9 in the dimensionless time if $a/b = 0.05$.

The effect of crystal size is also twofold. It is expected that, for a given melt inclusion, the larger its host crystal, the more difficult it is for the inclusion to reach equilibrium with the external melt (this is one of the points emphasized by Scowen et al., 1991). One might expect that the time (when used alone, time means dimensional time hereafter) it takes to reach a given extent of reequilibration is proportional to the square of the radius of the crystal. This is not so because the ratio a/b is decreasing as b increases, and this helps to reduce the difficulty of the exchange, as shown earlier. If both a and b are changing in such a way that a/b remains constant, then the time needed to reach a given degree of reequilibration is truly proportional to the square of the radius of the crystal. Relations for the case where a is constant and b is increasing are shown in Figure 6. For example, if $k = 10^{-3}$ and if the grain size increases by a factor of 5 while the inclusion size is the same, such that a/b decreases from 0.05 to 0.01, then to reach 50% of reequilibration takes about 6.5 times as long for the larger crystal as for the smaller crystal. This difference will generally decrease as the degree of reequilibration increases or as k decreases. Thus, the time it takes to reach 90% reequilibration for a k value of 10^{-3} will increase by a factor of 5 (compared to 6.5 for 50% reequilibration) if the crystal size increases by a factor of 5. This effect of crystal size on reequilibration time further reduces to a factor of ~1.1 with 90% reequilibration when k decreases to 10^{-4} with otherwise equal conditions.

In our treatment of the reequilibration problem, we assume inclusions to be in the centers of their host crystals. For an inclusion not in the center, the value of b is probably smaller than the host crystal radius but larger than the distance between the center of the inclusion and the closest rim of the crystal. A better constraint requires a numerical solution to the problem.

General applications

Reequilibration of H_2O between melt inclusions in quartz and external melt

Evaluation of reequilibration times requires knowledge of the diffusivity and partition coefficient of H_2O in quartz. Neither of these is certain.

Diffusivity of H_2O in quartz

Numerous attempts have been made to determine the diffusivity of H_2O-associated species in quartz because of its role in weakening quartz. The pioneer experimental study by Kats et al. (1962), using an IRS technique on the incorporation of OH in quartz, yielded the diffusivity of H_2O-associated species (OH^-, H^+, and H_2O) in quartz on the order of 10^{-10} to 10^{-7} cm²/s in the temperature range of 700–900 °C and at low pressures (<30 bars). This is supported by the studies of Blacic (1981) and Mackwell and Paterson (1985), who found the diffusivity of H_2O in quartz in the range of 10^{-9} to 10^{-7} cm²/s under the conditions of 800–900 °C and 15 kbar. On the other hand, Shaffer et al. (1974) found the diffusion coefficient of tritiated H_2O in β quartz to be about 10^{-13} cm²/s at 900 °C and low pressure. Kronenberg et al. (1986) and Gerretsen et al. (1989) also suggested low diffusivity of molecular H_2O in quartz, probably lower than 10^{-10} cm²/s, according to their experiments at 900 °C and 4–15 kbar. The diffusivity of H (as H^+) is much higher, on the order of 10^{-7} cm²/s under the above conditions. Rovetta et al. (1986, 1989) also obtained a diffusivity of 10^{-7} cm²/s for H species at 900 °C and 15 kbar in natural quartz crystals. They suggested that the diffusive incorporation of H species into quartz defect sites is probably followed by the reaction of these species with lattice O to form OH and H_2O molecules. It is our assessment from these studies that the diffusivity of bulk H_2O in quartz probably lies in the range of 10^{-10} to 10^{-7} cm²/s. Diffusivity as low as 10^{-13} cm²/s may also be possible.

Hall et al. (1991) suggested that postentrapment diffusional exchange of molecular H between fluid inclusions and the external fluid can significantly change the composition of the fluid inclusions. It is thus necessary to know if H_2 diffusion is also an important process in modifying the H_2O content of melt inclusions. Transport of H_2O by molecular H diffusion requires an f_{H_2} gradient, the maintenance of which is possible only if a reducing agent is available to reduce inclusion H_2O to H_2. The relatively large amount of H_2O and the small amount of FeO in natural rhyolitic melts thus relegates H_2O removal by H_2 loss to a negligible level. Consequently, mobility of H_2O through quartz in most natural rhyolitic environments probably will be determined by the diffusivity of H_2O, OH^-, and H^+, not by H_2. It is interesting to note that molecular H_2O, not OH^-, is believed to be the dominant diffusing species in rhyolitic glass (Zhang et al., 1991a). This is probably also the case for quartz (Zhang et al., 1991b).

It is important to note that the driving force for H_2O to diffuse is not its concentration gradient, but its activity gradient. Because the pressure within an inclusion can differ from the external pressure, the actual equilibrium concentration of H_2O in the respective melts can likewise differ. Computation based on Burnham (1979) shows that such a difference is small. For example, if the external pressure is 1500 bars and the internal pressure is 2000 bars, then the activity of H_2O will be the same both within and without if the H_2O content of the enclosed melt is about 10% higher than that of the external melt.

Partition coefficient of H_2O between quartz and melt

The equilibrium partition coefficient of H_2O between quartz and rhyolitic melt is poorly known. Watson et al. (1982) took the partition coefficient of H_2O between melt inclusion–bearing minerals and melt to be 0.001. This is probably an upper limiting value for quartz. The solubility of H_2O in quartz is controversial and is probably in the range of less than 100 H atoms/10^6 Si (corresponding to 15 ppm of H_2O by weight) to a few hundred H/10^6 Si at 700–900 °C and 3–15 kbar hydrothermal pressures (e.g., Mackwell and Paterson, 1985; Kronenberg et al., 1986; Rovetta et al., 1986, 1989; Gerretsen et al., 1989). The solubility of H_2O in quartz phenocrysts from rhyolitic glasses is unknown but is very likely to be less than that in hydrothermally annealing quartz. In other words, probably only a few parts per million of H_2O are present in quartz phenocrysts from rhyolites. As most rhyolitic melts contain a few wt% of H_2O, we thus tentatively take the partition coefficient to be about 0.0001.

Estimation of reequilibration time

The degree of reequilibration can be computed from Equation 12 as a function of the dimensionless time τ (= Dt/b^2), given the values of α (= a/b, the ratio of inclusion radius over host crystal radius) and k. The results show that, for $\alpha = 0.025$ (see Fig. 3), reaching 95% reequilibration takes about 5.5 in the dimensionless time if $k = 10^{-4}$, or about 11 if $k = 5 \times 10^{-5}$. Thus if the host crystal radius $b = 0.1$ cm and the melt inclusion radius $a = 25$ μm (such that $a/b = 0.025$) and if $D = 10^{-8}$ cm²/s, 64 d suffice to achieve 95% reequilibration when $k = 10^{-4}$, or about 130 d when $k = 5 \times 10^{-5}$. If D is 2 orders of magnitude smaller, the time will increase by 2 orders of magnitude, and this is still a geologically and volcanologically short interval of time. However, if D is as small as 10^{-13} cm²/s, as suggested by Shaffer et al. (1974), then the time can be as long as 10^4 yr, which, although still geologically short, is long in comparison to intervals between most volcanic eruptions from a single volcanic center. The preceding result is rather surprising. It implies that for many volcanic rocks, the H_2O concentration in a melt inclusion probably reflects partially or totally the H_2O concentration of the last intratelluric melt with which the crystal was in contact. The probable rapid reequilibration of H_2O between a melt inclusion and the external melt suggests that only melt inclusions from quickly cooled magmas such as air-fall materials can record the H_2O contents in a preerupted magma body. Melt inclusions in quartz from thick lava flows and welded ash flows may record H_2O concentrations that are significantly less than the original magmatic values because of posteruptive partial reequilibration.

As larger melt inclusions or melt inclusions located farther from the crystal surface reequilibrate more slowly (for inclusions not at the center of their host crystals, the

"radius" of the crystals may probably be approximated by the distance of the inclusions to crystal surfaces), it is expected that the H_2O concentration in melt inclusions will increase with increasing inclusion size and distance to crystal rim. Thus, in principle, by measuring the H_2O contents in various melt inclusions, it is possible to infer a cooling history for an ash or lava flow. Conversely, if the cooling history is known, then the variation in the H_2O content of melt inclusions could be used to assess the diffusivity and solubility of H_2O in quartz.

Chemical compositions of melt inclusions in minerals

The composition of melt inclusions in minerals have been used to assess the compositions of melts from which the crystals and their inclusions formed. Such inclusions form both within the crust and the upper mantle (see the review by Roedder, 1984) and in lunar rocks (Roedder and Weiblen, 1970) and even meteorites (e.g., Johnson et al., 1991). Commonly it is necessary to take into account the effect of dissolution from and precipitation onto the host crystals (Watson, 1976). Our results indicate that, in addition to the dissolution and precipitation, diffusive reequilibration with external melt may play an important role.

Consider LREEs in melt inclusions of clinopyroxene as an example. The partition coefficients of LREEs between clinopyroxene and basaltic melt are ~0.05 (Frey et al., 1978), and their diffusion coefficients in clinopyroxene are probably on the order of 10^{-12} to 10^{-14} cm^2/s at 1200–1300 °C (Hofmann and Hart, 1978; Sneeringer et al., 1984). Thus, for a clinopyroxene crystal 1 mm in radius with a melt inclusion 25 μm in radius located in the center of the crystal, it takes from 100 to 10000 yr (reflecting the range in diffusion coefficients) for the LREEs in the inclusion to reach 90% of reequilibration with external melt. On the other hand, for LREEs in inclusions within olivine, reequilibration time is longer, as LREEs are more incompatible in olivine. With 0.0005 as their partition coefficient, it takes from ~300 to 30000 yr to reach 90% reequilibration, when the same range of diffusion coefficient as for cpx is assumed. It seems that olivine and, probably, orthopyroxene as well better preserve the original concentrations of highly incompatible elements (e.g., Ba, Cs, Rb, Th, U, LREEs, etc.) in melt inclusions than does clinopyroxene. For a given melt inclusion, highly incompatible elements ($k \leq 0.001$) are better preserved than slightly incompatible elements ($k > \sim 0.1$) and compatible elements. For example, with the partition coefficient of Ni between olivine and melt in the range of 5–20 (Hart and Davis, 1978), it takes about 90 yr to reach 90% reequilibration for a melt inclusion with a 25-μm radius within a 1-mm olivine if the diffusion coefficient of Ni in olivine is 10^{-12} cm^2/s (or about 10 yr if $D = 10^{-11}$ cm^2/s). This is at least 3 times shorter than for a highly incompatible element (≥300 yr). The difference increases as the inclusion size increases. Thus, if the radii of an inclusion and its host crystal are 50 μm and 1 mm, respectively, then whereas it takes ~100 yr for a compatible element to reach 90% reequilibration, it takes ~1000 yr for an incompatible element with $k = 0.0005$ to reach the same degree of reequilibration, when a diffusivity of 10^{-12} cm^2/s for both elements in the host crystal is assumed. As a consequence, the concentration of a compatible element in a melt inclusion is expected to be modified to a higher degree by the external melt than for a concentration of a highly incompatible element.

It is interesting to reconsider the results of Scowen et al. (1991) in the light of our model (although our model is developed specifically for melt inclusions, its results can largely be applied to both fluid and mineral inclusions). Scowen et al. (1991) observed the reequilibration degree for different elements in chromite inclusions within olivines in the following order: $Mg \geq Fe^{2+} > Fe^{3+} \geq Al > Cr \geq Ti$. They used the difference in diffusion coefficient to explain this trend, suggesting the following diffusivity order in olivine: $Mg \approx Fe^{2+} > Al \approx Fe^{3+} \gg Cr \approx Ti$. We have shown that in addition to diffusivity, the difference in the partition coefficients will also affect the reequilibration rate. It is interesting to note that the difference in partition coefficients of the above elements in olivine are probably in the following order: $Mg \geq Fe^{2+} > Fe^{3+} \approx Cr \gg Al \approx Ti$. Note the similarity between the reequilibration order observed by Scowen et al. (1991) and the partition coefficient order.

Implications of H_2O contents of Bishop melt inclusions

The Bishop Tuff is a voluminous rhyolitic tuff (~600 km^3, Bailey et al., 1976; Izett et al., 1988) that erupted about 0.7 Ma (Dalrymple et al., 1965). Detailed studies indicate that the Bishop magma was zoned toward a less differentiated composition and a higher temperature with greater depth (Hildreth, 1977, 1979). Our recent work (Lu et al., 1990; Lu and Anderson, 1991) reveals that both the thermal and chemical gradients resulted from magma mixing caused by the addition of hotter, less differentiated magma to the deeper, late-erupted part of the Bishop magma at a late stage; before magma mixing, the late-erupted magma was similar to the early-erupted magma in major- and trace-element compositions and temperature.

Magma mixing changed the composition of the late-erupted melt, which, in turn, generated chemical potential differences between early-formed inclusions and the modified external melt. The difference in chemical potentials drove diffusion through the crystalline container of the inclusions. The amount of time available for diffusive reequilibration may be roughly equated with the duration of time from the beginning of magma mixing to the extrusion of the late-erupted Bishop magma. This time has been constrained to be at least several hundred years, based on probable diffusive equilibration of the early-formed titanomagnetite phenocrysts with the mixed magma (Lu, 1991).

Although many trace-element concentrations in late-erupted inclusions overlap those of early-erupted inclu-

sions (Lu, 1991), the H_2O concentrations in late-erupted inclusions are both less than those in early-erupted inclusions and remarkably constant: 20 inclusions range from 3.7 to 4.6 wt% and average 4.0 wt%, with a standard deviation of 0.2 wt%, which is close to the analytical uncertainty (Skirius, 1990; Skirius et al., 1990).

Uniform H_2O concentration in melt inclusions may reflect reequilibration of H_2O in the melt inclusions with the external melt, given the long residence time of the late-erupted magma after magma mixing. Therefore, the melt inclusions that were trapped before or at an early stage of magma mixing may have lost any indication of their original H_2O concentrations. Consequently, melt inclusions in the late-erupted Bishop Tuff, regardless of their time of formation, probably record only the H_2O concentration of the mixed magma shortly before eruption. As a consequence, their H_2O concentration may be decoupled from the trace-element concentrations that could not diffusively reequilibrate with the new magma because of smaller diffusivities or solubilities in quartz.

Applications to fluid inclusions

Diffusive reequilibration of fluid inclusions with external fluid during metamorphism has been of interest to many researchers (Roedder, 1981; Pasteris and Wanamaker, 1988; Hollister, 1988; Sterner et al., 1988; Hall and Bodnar, 1989; Mackwell and Kohlstedt, 1990; Hall et al., 1991). For example, CO_2-rich fluid inclusions in quartz from granulites, as well as in olivine from mantle xenoliths, may be explained by the preferential diffusive loss of H_2O out of the fluid inclusions (Roedder, 1981; Mackwell and Kohlstedt, 1990); changes in the f_{O_2} and f_{H_2} of the external fluids may result in a significant change in the composition of the fluid inclusions because of the diffusive exchange of O_2 and H_2 between the inclusions and the external fluids (Pasteris and Wanamaker, 1988; Hall et al., 1991).

Diffusive exchange of H_2O between fluid inclusions and external fluids is possible if the partial H_2O pressure of the fluid inclusions is different from that of the external fluids and if H_2O solubility in quartz varies with H_2O partial pressure. Consider a fluid inclusion trapped in a quartz crystal. If the P_{H_2O} of the external fluid is different from the P_{H_2O} of the fluid inclusion, then the H_2O concentration in the outer surface (in contact with the external fluid) will be different from the H_2O concentration in the inner surface (in contact with the fluid inclusion). As a consequence, a concentration gradient in H_2O within the crystal is formed, and H_2O will diffuse across the crystal, resulting in the modification of the composition of the fluid inclusion.

Following the treatment of melt inclusions, we define the diffusive reequilibration degree (Φ) for fluid inclusion as: $\Phi(t) = [P_i(t) - P_0]/(P_e - P_0)$, where $P_i(t)$ is the P_{H_2O} in the inclusion, P_0 is the P_{H_2O} in the inclusion before diffusive exchange, and P_e is the P_{H_2O} of the external fluid. It can be formally shown that $\Phi(t)$ has the same expression as $\phi(t)$, i.e., Equation 12, except that β is defined differently:

$$\beta = 3\rho_c \kappa R T/M \tag{15}$$

where ρ_c is the density of quartz, R the gas constant, T the temperature, M the molecular weight of H_2O, and κ the solubility coefficient of H_2O in quartz defined as $\kappa = C/P_{H_2O}$, in which C is the concentration of H_2O in quartz in equilibrium with a partial H_2O pressure of P_{H_2O}. The solubility coefficient κ is not well constrained. Spear and Selverstone (1983) inferred a κ value of about 25 ppm/kbar. This is probably too high because later studies have revealed a significantly lower solubility of H_2O in quartz (e.g., Kronenberg et al., 1986; Rovetta et al., 1986, 1989; Gerretsen et al., 1989). The solubility is probably only a few parts per million at 3 kbar and 700–900 °C to over 10 ppm at 15 kbar and the same temperatures. This implies a κ value of about 1 ppm/kbar. Thus, at 500 °C, β is equal to 2.9×10^{-5}, based on Equation 15.

As an application of the diffusive reequilibration model to fluid inclusions, consider the following case: three fluid inclusions with radii of 10, 25, and 50 μm are trapped at the centers of quartz crystals 1 mm in radius from a metamorphic rock under the conditions of 8 kbar and 500 °C. The compositions of the fluid inclusions are 80% H_2O and 20% CO_2 (by mole) initially. Now suppose that this metamorphic rock is uplifted virtually isothermally and the pressure drops to 3 kbar, while the temperature remains at 500 °C. Under this circumstance, the pressure within the inclusions remains unchanged (= 8 kbar), and the partial H_2O pressure is 6.4 kbar; outside the crystals, P_{H_2O} = 2.4 kbar, if the external fluid is still 80% H_2O and 20% CO_2. As the internal P_{H_2O} is higher than the external P_{H_2O}, H_2O will diffuse out of the fluid inclusions. The reequilibration degrees and the pressure and the compositional changes within these inclusions can be computed from Equation 12, with $\beta = 2.9 \times 10^{-5}$. The results are presented in Table 2. In calculating the $CO_2/(CO_2 + H_2O)$ ratio, it is assumed that diffusive leakage of CO_2 is negligible. This is probably a reasonable assumption because both the solubility and diffusivity of CO_2 in quartz are expected to be much smaller than for H_2O.

It can be seen from Table 2 that, because of the diffusive loss of H_2O out of the inclusions during retrograde metamorphism, the $CO_2/(H_2O + CO_2)$ ratio increases significantly for inclusions smaller than 25 μm in radius, if the external pressure drops to and remains at 3 kbar for 100 000 yr while the temperature remains at 500 °C. In fact, for inclusions 10 μm and smaller in radius trapped in a 1-mm quartz crystal, less than 50000 yr is needed to reequilibrate the inclusions completely. On the other hand, for large fluid inclusions ($\geq$50 μm in radius), at least about 10^6 yr is required to reequilibrate the inclusions completely.

Host crystals may crack if the internal pressure is significantly higher than the external pressure (Tait, 1992), thus resulting in the rapid leakage of both H_2O and CO_2 along the cracks. However, crystals serving as hosts for small inclusions (smaller than 25 μm) may not crack be-

TABLE 2. Diffusive leakage of H_2O from fluid inclusions in quartz during retrograde decompressional metamorphism

	After 10000 yr			After 100000 yr		
a (μm)*	Φ (%)*	P_{H_2O} (kbar)*	$\frac{CO_2}{CO_2 + H_2O}$*	Φ (%)*	P_{H_2O} (kbar)*	$\frac{CO_2}{CO_2 + H_2O}$*
10	60	4.0	0.29	100	2.4	0.40
25	15	5.8	0.22	75	3.4	0.32
50	5	6.2	0.21	30	5.2	0.24

Note: Host crystal radius = 1 mm. The initial total pressure within the inclusions is 8 kbar. Initial partial H_2O pressure = 6.4 kbar. The diffusivity of H_2O in quartz at 500 °C = 10^{-13} cm²/s, obtained by taking $D = 10^{-9}$ cm²/s at 800 °C and an activation energy of 200 kJ/mol.

* The letter a is the inclusion radius; Φ is the reequilibration degree; P_{H_2O} is the partial H_2O pressure in the fluid inclusions; $CO_2/(H_2O + CO_2)$ is the molar ratio, which equals 0.2 prior to the diffusive loss of H_2O.

cause the uplift and decompression of metamorphic rocks generally proceed very slowly, in the time scale of 10^6 yr, whereas diffusive loss of H_2O from small fluid inclusions to the point of equilibrium with external fluid can be accomplished in less than 10^5 yr, thereby reducing the difference between internal and external pressure. For larger fluid inclusions, diffusive loss of H_2O can be less significant, with consequent cracking in the host crystals. It follows that a study of the composition and size of fluid inclusions may help constrain the uplift history.

Summary and conclusions

This study provides a theoretical treatment of the diffusive reequilibration of both melt and fluid inclusions at constant temperature. It allows a quantitative evaluation of the roles of various parameters in controlling the reequilibration rate. Reequilibration of a chemical species in an inclusion with external melt or fluid depends on (1) the diffusivity (D) of the species in the host crystal; (2) inclusion size (a); (3) host crystal size (b); and (4) partition coefficient (k) of the species between crystal and melt or fluid. The reequilibration degree decreases as D and k decrease and as a and b increase. Reequilibration of H_2O in a melt inclusion in quartz with external melt is probably geologically rapid at temperatures relevant to rhyolitic melts (700–800 °C) because of the high diffusivity of H_2O in quartz. As a consequence, the original H_2O content in a melt inclusion is unlikely to be preserved. For fluid inclusions, even though the solubility of H_2O in quartz is quite low (~1 ppm/kbar P_{H_2O}), diffusive leakage of H_2O from small fluid inclusions ($\leq$10 μm in radius) in quartz from metamorphic rocks can be significant during the slow uplifting of the metamorphic rocks, resulting in an increase in the $CO_2/(H_2O + CO_2)$ ratio in the inclusions.

Because diffusive reequilibration also depends on the partition coefficient, the original concentrations of highly incompatible elements in inclusions are probably better preserved than those of moderately incompatible elements and compatible elements. This has two direct consequences: different elements in the same inclusion exchange with external melt to different degrees; the same elements in melt inclusions trapped in different host minerals (e.g., cpx vs. olivine) may reequilibrate differently.

Acknowledgments

Constructive comments by E.B. Watson and C.R. Bacon are gratefully acknowledged. We thank V. Barcilon and J.R. Goldsmith for helpful comments on an earlier version of the manuscript. This work was supported by NSF EAR-8905081 to M.C. Monaghan, and EAR-8904070 to A.T.A.

References cited

Albarede, F., and Bottinga, Y. (1972) Kinetic disequilibrium in trace element partitioning between phenocrysts and host lava. Geochimica et Cosmochimica Acta, 36, 141–156.

Anderson, A.T. (1974) Evidence for a picritic volatile-rich magma beneath Mt. Shasta, California. Journal of Petrology, 15, 243–267.

——(1976) Magma mixing: Petrological process and volcanological tool. Journal of Volcanology and Geothermal Research, 1, 3–33.

Anderson, A.T., and Wright, T.L. (1972) Phenocrysts and glass inclusions and their bearing on oxidation and mixing of basaltic magmas, Kilauea volcano, Hawaii. American Mineralogist, 57, 188–216.

Bacon, C.R. (1989) Crystallization of accessory phases in magmas by local saturation adjacent to phenocrysts. Geochimica et Cosmochimica Acta, 53, 1055–1066.

Bailey, R.A., Dalrymple, G.B., and Lanphere, M.A. (1976) Volcanism, structure, and geochronology of Long Valley Caldera, Mono County, California. Journal of Geophysical Research, 81, 725–744.

Blacic, J.D. (1981) Water diffusion in quartz at high pressure: Tectonic implications. Geophysical Research Letters, 8, 721–723.

Burnham, C.W. (1979) The importance of volatile constituents. In H.S. Yoder, Ed., The evolution of igneous rocks—Fiftieth anniversary perspectives, p. 439–482. Princeton University Press, Princeton, New Jersey.

Carslaw, H.S., and Jaeger, J.C. (1959) Conduction of heat in solids. Clarendon Press, London.

Dalrymple, G.B., Cox, A., and Doell, R.R. (1965) Potassium-argon age and paleomagnetism of the Bishop Tuff, California. Geological Society of American Bulletin, 76, 665–673.

Frey, F.A., Green, D.H., and Ray, S.D. (1978) Integrated models of basalt petrogenesis: A study of quartz tholeiites to olivine melilitites from southeastern Australia utilizing geochemical and experimental petrological data. Journal of Petrology, 19, 463–513.

Gerretsen, J., Paterson, M.S., and McLaren, A.C. (1989) The uptake and solubility of water in quartz at elevated pressure and temperature. Physics and Chemistry of Minerals, 16, 334–342.

Hall, D.L., and Bodnar, R.J. (1989) Methane in fluid inclusions from granulites: A product of hydrogen diffusion? Geochimica et Cosmochimica Acta, 54, 641–651.

Hall, D.L., Bodnar, R.J., and Craig, J.R. (1991) Evidence for postentrapment diffusion of hydrogen into peak metamorphic fluid inclusions from the massive sulfide deposits at Ducktown, Tennessee. American Mineralogist, 76, 1344–1355.

Hart, S.R., and Davis, K.E. (1978) Nickel partitioning between olivine and silicate melt. Earth and Planetary Science Letters, 40, 203–219.

Hildreth, E.W. (1977) The magma chamber of the Bishop Tuff: Gradients in temperature, pressure and composition. Ph.D. thesis, University of California, Berkeley, California.

——(1979) The Bishop Tuff: Evidence for the origin of the compositional zonation in silicic magma chambers. Geological Society of America Special Paper, 180, 43–76.

Hofmann, A.W., and Hart, S.R. (1978) An assessment of local and regional isotopic equilibrium in the mantle. Earth and Planetary Science Letters, 38, 44–62.

Hollister, L.S. (1988) On the origin of CO_2-rich fluid inclusions in migmatites. Journal of Metamorphic Geology, 6, 467–474.

Izett, G.A., Obradovich, J.D., and Mehnert, H.H. (1988) The Bishop ash bed (middle Pleistocene) and some older (Pliocene and Pleistocene)

chemically and mineralogically similar ash beds in California, Nevada, and Utah. U.S. Geological Survey Bulletin, 1675, 1–37.

Johnson, M.C., Rutherford, M.J., and Hess, P.C. (1991) Chassingy petrogenesis: Melt compositions, intensive parameters, and water contents of martian (?) magmas. Geochimica et Cosmochimica Acta, 55, 349–366.

Karsten, J.L., Holloway, J.R., and Delaney, J.R. (1982) Ion microprobe studies of water in silicate melts: Temperature-dependent water diffusion in obsidian. Earth and Planetary Science Letters, 59, 420–428.

Kats, A., Haven, Y., and Stevels, J.M. (1962) Hydroxyl groups in β-quartz. Physics and Chemistry of Glasses, 3, 69–75.

Kronenberg, A.K., Kirby, S.H., Aines, R.D., and Rossman, G.R. (1986) Solubility and diffusional uptake of hydrogen in quartz: Implications for hydrolytic weakening. Journal of Geophysical Research, 91, 12723–12744.

Lapham, K.E., Holloway, J.R., and Delaney, J.R. (1984) Diffusion of H_2O and D_2O in obsidian at elevated temperatures and pressures. Journal of Non-Crystalline Solids, 67, 179–191.

Lu, F. (1991) The Bishop Tuff: Origin of the high-silica rhyolite and its thermal and compositional zonations. Ph.D. dissertation, University of Chicago, Chicago, Illinois.

Lu, F., and Anderson, A.T. (1991) Mixing origins of volatile and thermal gradients in the Bishop magma. Eos, 72, 312.

Lu, F., Anderson, A.T., and Davis, A.M. (1990) Implications of glass inclusions for the origins of high silica rhyolite and compositional zonation of the Bishop Tuff, California. Eos, 71, 651.

Mackwell, S.J., and Kohlstedt, D.L. (1990) Diffusion of hydrogen in olivine: Implications for water in the mantle. Journal of Geophysical Research, 95, 5079–5088.

Mackwell, S.J., and Paterson, M.S. (1985) Water related diffusion and deformation effects in quartz at pressures of 1500 and 300 MPa. In R.N. Schock, Ed., Point defects in minerals, monograph 31, p. 141–150. Washington, D.C.

Pasteris, J.D., and Wanamaker, B.J. (1988) Laser microprobe analysis of experimentally re-equilibrated fluid inclusions in olivine: Some implications for mantle fluids. American Mineralogist, 73, 1074–1088.

Roedder, E. (1981) Origin of fluid inclusions and changes that occur after trapping. In L.S. Hollister and N.L. Crawford, Eds., Short course in fluid inclusions: Applications to petrology, p. 103–137. Mineralogical Association of Canada, Calgary.

——— (1984) Fluid inclusions. In Mineralogical Society of America Reviews in Mineralogy, 12, 644 p.

Roedder, E., and Weiblen, P.W. (1970) Lunar petrology of silicate melt inclusions, Apollo 11 rocks. Proceedings of Apollo 11 Lunar Science Conference, 1, 801–837.

Roeder, P.L., and Campbell, I.H. (1985) The effects of postcumulus reactions on composition of chrome-spinels from the Jimberlana intrusion. Journal of Petrology, 26, 763–786.

Rovetta, M.R., Holloway, J.R., and Blacic, J.D. (1986) Solubility of hydroxyl in natural quartz annealed in water at 900 °C and 1.5 GPa. Geophysical Research Letters, 13, 145–148.

Rovetta, M.R., Blacic, J.D., Hervig, R.L., and Holloway, J.R. (1989) An experimental study of hydroxyl in quartz using infrared spectroscopy and ion microprobe techniques. Journal of Geophysical Research, 94, 5840–5850.

Scowen, P.A.H., Roedder, P.L., and Helz, R.T. (1991) Reequilibration of chromite within Kilauea Iki lava lake, Hawaii. Contributions to Mineralogy and Petrology, 107, 8–20.

Shaffer, E.W., Sany, J.S., Cooper, A.R., and Heuer, A.H. (1974) Diffusion of tritiated water in β-quartz. Carnegie Institution of Washington Publication 634, 131–138.

Skirius, C.M. (1990) Pre-eruptive H_2O and CO_2 content of the plinian and ash-flow Bishop Tuff magma. Ph.D. dissertation, University of Chicago, Chicago, Illinois.

Skirius, C.M., Peterson, J.W., and Anderson, A.T. (1990) Homogenizing silicate glass inclusions. American Mineralogist, 75, 1381–1398.

Sneeringer, M.A., Hart, S.R., and Shimizu, N. (1984) Strontium and samarium diffusion in diopside. Geochimica et Cosmochimica Acta, 48, 1589–1608.

Spear, F.S., and Selverstone, J. (1983) Water exsolution from quartz: Implications for the generation of retrograde metamorphic fluids. Geology, 11, 82–85.

Sterner, S.M., Hall, D.L., and Bodnar, R.J. (1988) Post-entrapment compositional changes in fluid inclusions: Experimental evidence for water diffusion in quartz. Geological Society of America Abstracts with Programs, 20, A100.

Tait, S. (1992) Selective preservation of melt inclusions in igneous phenocrysts. American Mineralogist, 77, 146–155.

Watson, E.B. (1976) Glass inclusions as samples of early magmatic liquid: Determinative method and application to a south Atlantic basalt. Journal of Volcanology and Geothermal Research, 1, 73–84.

Watson, E.B., Sneeringer, M.A., and Ross, A. (1982) Diffusion of dissolved carbonate in magmas: Experimental results and applications. Earth and Planetary Science Letters, 61, 346–358.

Zhang, Y., Stolper, E.M., and Wasserburg, G.J. (1991a) Diffusion of water in rhyolitic glasses. Geochimica et Cosmochimica Acta, 55, 441–456.

——— (1991b) Diffusion of a multi-species component and its role in oxygen and water transport in silicates. Earth and Planetary Science Letters, 103, 228–240.

Manuscript received June 10, 1991
Manuscript accepted January 9, 1992

Appendix 1. Solution of the diffusive reequilibration problem

The two variables t and r can be made nondimensionalized by letting $\tau = Dt/b^2$ and $x = r/b$. With these, Equation 2 coupled with its initial condition (Eq. 3) and boundary conditions (Eqs. 4 and 6) takes the following dimensionless forms:

$$\frac{\partial C}{\partial \tau} = \frac{\partial^2 C}{\partial x^2} + \frac{2}{x}\frac{\partial C}{\partial x}, \qquad \alpha < x < 1 \tag{A1}$$

where $\alpha = a/b$.

The initial condition is

$$C(x,0) = kC_0, \qquad \alpha \le x \le 1. \tag{A2}$$

The two boundary conditions are

$$C(1,\tau) = kC_e \tag{A3}$$

$$\frac{dC(\alpha,\tau)}{d\tau} = (\beta/\alpha)\frac{\partial C}{\partial x}\Big|_{x=\alpha}. \tag{A4}$$

The Laplace transformation method can be used to solve this problem. Denote the Laplace transformation of $C(x,t)$ and $\hat{C}(x,p)$; i.e.,

$$\hat{C}(x,p) = \int_0^\infty C(x,\tau)\exp(-p\tau)\, d\tau. \tag{A5}$$

The Laplace transformation of Equation A1 is

$$p\hat{C} - kC_0 = \frac{d^2\hat{C}}{dx^2} + \frac{2}{x}\frac{d\hat{C}}{dx} \qquad \alpha < x < 1. \tag{A6}$$

The general solution of Equation A6 is

$$\hat{C}(x,p) = \frac{1}{x}(Ae^{\lambda x} + Be^{-\lambda x}) + \frac{kC_0}{p} \tag{A7}$$

where A and B are constants to be determined from the two boundary conditions and $\lambda = \sqrt{p}$.

The Laplace transformation of Equation A3 is $\hat{C}(1,p) = kC_e/p$, which, when considering Equation A7, becomes

$$Ae^{\lambda} + Be^{-\lambda} = \delta/p \tag{A8}$$

where

$$\delta = k(C_e - C_0). \tag{A9}$$

Applying the Laplace transformation to Equation A4 gives

$$p\hat{C}(\alpha,p) - kC_0 = (\beta/\alpha)\frac{d\hat{C}}{dx}|_{x=\alpha}.$$

Substituting this into Equation A7 yields

$$A(\beta + \alpha^2 p - \alpha\beta\lambda)e^{\lambda\alpha} + B(\beta + \alpha^2 p + \alpha\beta\lambda)e^{-\lambda\alpha} = 0. \tag{A10}$$

Equations A8 and A10 can be solved simultaneously to give A and B:

$$A = \frac{\delta}{2Qp}(\beta + \alpha^2 p + \alpha\beta\lambda)e^{-\lambda\alpha} \tag{A11a}$$

$$B = \frac{\delta}{2Qp}(\beta + \alpha^2 p - \alpha\beta\lambda)e^{\lambda\alpha} \tag{A11b}$$

where

$$Q = (\beta + \alpha^2 p)\sinh(1-\alpha)\lambda + \alpha\beta\lambda\cosh(1-\alpha)\lambda. \tag{A11c}$$

Therefore,

$$\hat{C}(x,p) = \frac{kC_0}{p} + \frac{1}{x}\frac{\delta}{Qp}[(\beta + \alpha^2 p)\sinh(x-\alpha)\lambda + \alpha\beta\lambda\cosh(x-\alpha)\lambda]. \tag{A12}$$

$C(x,\tau)$ can now be obtained by applying the inverse Laplace transformation to $\hat{C}(x,p)$; i.e.,

$$C(x,\tau) = \frac{1}{2\pi i}\int_{-i\infty}^{i\infty}\hat{C}(x,p)\exp(p\tau)\,dp. \tag{A13}$$

This integral on the complex plane can be evaluated by the residue theory. Note that $\hat{C}(x,p)$ is a single-valued function of p, even though λ ($= \sqrt{p}$) takes two values, one positive, the other negative, for any given p on the p complex plane. This is because $\hat{C}(x,p)$ is an even function of λ. Therefore, there is no branch point for the integral.

There is a pole at $p = 0$, with a residue of

$$R_0 = kC_0 + \frac{\delta}{x}\frac{\beta(x-\alpha) + \alpha\beta}{\beta(1-\alpha) + \alpha\beta} = kC_e. \tag{A14}$$

Other poles occur at $Q = 0$, or

$$(\beta + \alpha^2 p)\sinh(1-\alpha)\lambda + \alpha\beta\lambda\cosh(1-\alpha)\lambda = 0. \tag{A15}$$

There is an infinite number of negative roots of p (and thus imaginary roots of $\lambda = \sqrt{p}$) that satisfy Equation A15:

$$p = -q_n^2 \qquad (n = 1, 2, 3, \ldots) \tag{A16}$$

where the q's are the positive roots of

$$(\beta - \alpha^2 q^2)\sin(1-\alpha)q + \alpha\beta q\cos(1-\alpha)q = 0. \tag{A17}$$

This transcendental equation can be solved numerically. The first six roots for selected values of α and β have been compiled in Table 1.

The residue at $p = -q_n^2$ and $\lambda = iq_n$ is

$$R_n = \frac{\delta}{x}\frac{m_n}{M_n}\exp(-q_n^2\tau), \qquad n = 1, 2, 3, \ldots \tag{A18}$$

where

$$M_n = p\frac{dQ}{dp} \quad \text{at } p = -q_n^2 \quad \text{and } \lambda = iq_n$$
$$= -iq_n^2\{\alpha[\alpha + \beta(1-\alpha)/2]\sin(1-\alpha)q_n + \frac{1}{2q_n}[\alpha^2(1-\alpha)q_n^2 - \beta]\cos(1-\alpha)q_n\} \tag{A19}$$

$$m_n = i[(\beta - \alpha^2 q_n^2)\sin(x-\alpha)q_n + \alpha\beta q_n\cos(x-\alpha)q_n]$$
$$= i\alpha\beta q_n\frac{\sin(1-x)q_n}{\sin(1-\alpha)q_n} \tag{A20}$$

where Equation A17 has been used. And, finally,

$$C(x,\tau) = kC_e + \frac{2\beta k}{x}(C_0 - C_e) \times \sum_{n=1}^{\infty}\frac{\sin(1-x)q_n\exp(-q_n^2\tau)}{[\gamma q_n\sin^2(1-\alpha)q_n + (\tfrac{1}{2})[\alpha(1-\alpha)q_n^2 - \beta/\alpha]\sin 2(1-\alpha)q_n]} \tag{A21}$$

where $\gamma = 2\alpha + \beta(1-\alpha)$; $\alpha = a/b$; $x = r/b$; $\tau = Dt/b^2$.

The denominator in the summation in Equation A21 can be further manipulated by using Equation A17 so that it takes a form similar to that used by Carslaw and Jaeger (1959, p. 350, Eq. 24) for their special case. This is

$$C(x,t) = kC_e + \frac{4\beta k}{x}(C_0 - C_e) \times \sum_{n=1}^{\infty}\frac{\sin(1-x)q_n\exp(-q_n^2\tau)}{[2\beta(1-\alpha)q_n + 4\alpha q_n\sin^2(1-\alpha)q_n - \beta\sin 2(1-\alpha)q_n]}. \tag{A22}$$

It is more convenient to use Equation A21 when the composition of the melt inclusion is evaluated. The composition of the melt inclusion is

$$C_1(\tau) = C_e + \frac{2\beta}{\alpha}(C_0 - C_e) \times \sum_{n=1}^{\infty}\frac{\exp(-q_n^2\tau)}{\{\gamma q_n\sin[(1-\alpha)q_n] + [\alpha(1-\alpha)q_n^2 - \beta/\alpha]\cos[(1-\alpha)q_n]\}}. \tag{A23}$$